Received: 1 November 2021 | Revised: 16 February 2022 | Accepted: 21 February 2022

DOI: 10.1002/biot.202100587

Biotechnology Journal

RESEARCH ARTICLE

A highly sensitive PNA-microarray system for miRNA122 recognition

Giuseppe Forte[1] | **Giorgio Ventimiglia**[2] | **Massimiliano Pesaturo**[3] | **Salvatore Petralia**[1]

[1]Department of Drug Science and Health, University of Catania, Catania, Italy

[2]EM Microelectronic, Marin-Epagnier, Switzerland

[3]STMicroelectronics srl, Agrate Brianza, Italy

Correspondence
Giuseppe Forte and Salvatore Petralia, Department of Drug Science and Health, University of Catania, via S. Sofia 64, 95125 - Catania, Italy.
Email: salvatore.petralia@unict.it and gforte@unict.it

Abstract

Surface chemistry is a fundamental aspect of the development of the sensitive biosensor based on microarray technology. Here, an advanced PNA-microarray system for the detection of miRNA, composed by a multilayered Si/Al/Agarose component, is described. A straightforward optical signal enhancement is achieved thanks to a combination of the Al film mirror effect and the positive interference for the emission wavelength of the Cy5 fluorescent label tuned by the agarose film. The PNA-microarray was investigated for the detection of miRNA_122, resulting in a sensitivity of about 1.75 μM^{-1} and Limit of Detection in the range of 0.043 nM as a function of the capture probe sequence. The contribution, in terms of H-bonds amounts at 298 and 333 K, of the agarose coating to the dsPNA-RNA interactions was demonstrated by Molecular Dynamic simulations. These results pave the way for advanced sensing strategies suitable for the environmental monitoring and the public safety.

KEYWORDS
agarose surface, biosensor, miRNA, PNA-microarray hybridization

1 | INTRODUCTION

In the last decades, molecular diagnostic techniques have increased their utility in clinical, microbiology, and biology laboratories[1,2] for various applications such as genotyping, pharmacogenomics, and infectious pathogen disease.[3–6] The main features requested for diagnostics systems are the ability to detect and identify more than one target simultaneously, good sensitivity, easy-to-use, high accuracy in response, cost effective analysis, and fast response time.[7] In this scenario, the ability of nucleic acid microarrays to allow comprehensive simultaneous detection of thousands of sequences has resulted in the success of this technology in the molecular diagnostic area. Although molecular biology techniques such as quantitative real time polymerase chain reaction (RT-qPCR), isothermal PCR and Next Generation Sequencing are largely increasing their diffusion also in point of care format[8,9] microarrays is still a gold technology for nucleic acid testing.[10]

The microarray is an array of capture probes (including nucleic acids, proteins, carbohydrates, tissues, cells, polymers, etc.) immobilized on a chemically functionalized substrate, suitable for the detection of specific targets. The DNA-microarrays intended for nucleic acid detection are the most common and diffused systems, where a specific nucleic acid target can be recognized by hybridization with a DNA probe containing complementary sequences and anchored on the substrate's surface.

The chemistry of surface coating is one of the most relevant key factors of effectiveness in the microarray detection methodology.[11,12] Typically, hydroxyl-enriched surfaces such as glass, silicon oxide, quartz, and oxidized polymeric surfaces can be successfully modified, with carboxyl, aldehydic, amino, or epoxy terminated layers forming a reactive finished layer allowing the immobilization of specific probes at surface level, through covalently or electrostatically binding modes.[13] The passivation step is an additional process required to reduce the nonspecific binding of specific target with the surface, typically introduced to increase the signal/background ratio value and, as consequence, to improve the sensitivity. In this scenario, thanks to

Abbreviations: Cy5, cyanine 5; MA, Microarray; miRNA, micro RNA; PNA, peptide Nucleic acids; RT-qPCR, quantitative real time polymerase chain reaction

its attitude to form thermo-reversible gels in hot water and to its good biocompatibility, the agarose is a straightforward green-chemistry candidate for the preparation of microarray substrates for nucleic acids recognition,[14] protein detection,[15] and cells interrogation.[16]

MicroRNAs (miRNAs) are small noncoding RNA molecules, consisting of ≈20–22 nucleotides, involved in various cellular and physiological processes. Circulating miRNAs are present in biological fluids where their presence in variable concentration could be associated as biomarker with various diseases including cancer,[17] cardiovascular disease,[18] and metabolic disorders.[19] Although this approach is limited by some crucial drawbacks including preanalysis degradation of miRNA, matrix effects, variability in the extraction of microRNAs from plasma or serum, the RT-qPCR is the gold standard method for circulating microRNA quantification.[20]

The microRNA-122 (miR-122 and miR-122-5p) are highly expressed and specific for hepatocytes (≈40,000 copies per hepatocyte), with little or no expression in other tissues. The recognition of miR-122 is important because it has an active role in liver inflammation, as well as its vital role in promoting hepatitis B virus[21] and hepatitis C virus[22] suggesting the use of miRNA as promising marker for liver injury. In patients with acute liver injury, it was reported that the circulating concentration of miR-122 is increased 100–1000 fold compared to controls.[23]

In this scenario, the microarray hybridization approach is still one the most robust method for the detection of nucleic acids, where the target molecules, including miRNAs, are recognized by the specific probes. The structures of the capture probe are crucial for the assay sensitivity. The 20–22 mer long oligonucleotides of DNA (Deoxyribonucleic acid) and PNA (Peptide Nucleic Acids) are the most diffused capture probes. PNA are synthetic oligopeptides with nucleobases attached as sidechains, able to form stable hybrid duplex structures with complementary DNA or RNA sequences,[24,-25] largely for nucleic acid detection in lab on chip format.[14] Recently, Zhang and coworkers report a universal microarray platform based on DNA tetrahedral structured probe and hybridization chain reaction for a highly specificity and ultrasensitivity DNA and miRNA target detection.[26]

Herein we describe a novel miRNA recognition strategy based on a PNA-microarray printed on agarose film deposed on Si-Al layers for an effective optical signal enhancement. The use of agarose as an eco-friendly chemical guarantees a biocompatible finishing coating, a low cost and easy spin-coating preparation method. The coating was fully characterized by electron microscopy and optical techniques. This approach might pave the way to future developments of advanced miniaturized miRNA biosensor devices.

2 | EXPERIMENTAL SECTION

2.1 | Chemicals and materials

The agarose, periodic acid, sodium borohydride, saline disodium phosphate, SDS, and deionized water were purchased by Sigma-Aldrich and used as received. The substrates for microarray have been prepared by STMicroelectronics in clean room environment. The substrate was manufactured by standard VLSI technology and consists of a silicon 8′ wafer support and a mirror layer made of Al layer deposed by CVD method with thickness of about 700–800 nm.

The 5′ aminomodified PNA probe, was purchased by MWG (Germany) and used as received, at final concentration of 10 μM in 0.15 M phosphate buffer at pH 9.2 adding 0.01% w/v of SDS as printing additive. The reagents for passivation process and hybridization reaction were purchased by Sigma Aldrich and used as received. The Nexterion Aldehydesilane glass slides were purchased by Schott.

2.2 | Agarose coating preparation

The substrates were dipped in ethanol and cleaned in ultrawave bath at room temperature per 10 min, then rinsed in ethanol and dried by nitrogen flow. After that, a volume of 500 μl of preheated (65°C) aqueous agarose solution (1% w/v) was spread-out onto substrate surface to form the agarose coating, by spin-coating method with a speed ranging from 300 to 1000 rpm for 60 s. The agarose thickness was measured by SEM analysis of the cross-profile section. The agarose coated substrates were dried under vacuum overnight and stored at room temperature before the use.

2.3 | PNA microarray fabrication

Before PNA-microarray printing, the agarose coated substrates were activated by immersion in 10 mmol L^{-1} $NaIO_4$ in 0.1 mol L^{-1} phosphate buffer (pH 7.2) for 30 min at room temperature, then thoroughly rinsed with deionized distilled water and dried. The microarray was stored under nitrogen at 4°C before the use.

A 6 row × 4 column PNA-microarray (24 spots with size ≈150 μm) was printed on the activated agarose surface. After spotting the substrates were incubated for 4 h at 40°C and relative humidity of 90%. Later, the substrates have been immersed in aqueous $NaBH_4$ solution (1 mM), to chemically reduce the Schiff's base to amine group. Then, the slides were rinsed with distilled water and dried with nitrogen flow and ready for hybridization tests.

The PNA microarray probe sequences (specific for miRNA_122, positive and negative controls) are reported in table 1.

2.4 | Hybridization experiments

The microarray hybridization reactions were performed at 55°C for 60 min, using Cy5 labeled perfect matches specific for miRNA_122, at various target concentrations (0, 0.1, 0.5, 5, 10, 25, 50, and 200 nM) and perfect-match positive control at concentrations of 50 and 200 nM. The sequence of perfect matches target are reported in Table 1. After that, the substrates were washed by 2X SSC 0.2X SSC solution for 5 min under stirring at 40°C. Hybridization image acquisition and image analysis were performed by Scan-express instrument and software

TABLE 1 Microarray probe and perfect-match target sequences

Type	Name	Sequence 5t'-3t'
Probe/Specific PNA Probe	PNA_miRNA_122	NH_2-C_6-CAA ACA CCA TTG TCA CAC TCCA
Probe/Specific DNA Probe	DNA_ miRNA_122	NH_2-C_6-CAA ACA CCA TTG TCA CAC TCCA
Probe/PNA Positive controls	Pos_CTRL	NH_2-C_6-GCA GAG CCA TCT ATT GCT TAC
Probe/PNA Negative controls	Neg_CTRL	NH_2-C_6-AAA AAA AAA AAA AAA AAA AAA
Target/DNA Positive control	PM_Pos_CTRL	Cy5-GTA AGC AAT AGA TGG CTC TGC
Target/Perfect-Match miRNA_122	PM_ miRNA_122	Cy5-UGGA GUG UGA CAA UGG UGU UUG
Mismatch target	Mis-target	Cy5-CAC CAC CAC CAC CAC CAC CAC

supplied both by Perkin Elmer. The specificity tests were performed interrogating the microarray using specific target (pos_CTRL, miRNA_122) and unspecific targets (Mis-target) at concentration of 200 nM.

2.5 | Statistical analysis

Statistical analyses were performed by SPSS, IBM statistic subscription (Statistical Program for Social Science). The level of significant was set at $p < 0.05$. The measurement data were expressed as mean ± standard deviation (SD).

2.6 | Association constant (K_{ass}) assessment

The K_{ass} between the miRNA_122 target and the specific PNA probe was calculated by Langmuir isotherm model using Equation (1).

$$\frac{I}{I_{max} - I} = Ct\, x\, K_{ass.} \quad (1)$$

where I is the signal intensity, I_{max} is the maximum intensity at saturation condition, **Ct** is the miRNA molar concentration, and K_{ass} is the association constant. This standard model is valid for low target concentration, in the presence of impenetrable surface and in the absence of hybridization on bulk.[27] The K_{ass} assessment has been performed recording the fluorescence signal after miRNA_122 recognition experiments with various target concentration (0.0, 0.1, 0.5, 5.0, and 10.0 nM).

2.7 | Molecular Dynamic (MD) simulations

The structure of agarose was built starting from the disaccharide agarobiose, which was replicated by means of Build polymer tools included in the Biovia Material Studio 2017 package, setting the chain length and the number of chains to 20, so that the dimensions of the obtained 3D structure were 7.30 × 4.49 × 2.01 nm. Double strands consisted of PNA-RNA and DNA-RNA models were built employing the Discovery Studio 2019 package by using the PM_ miRNA_122 sequence reported in Table 1. The complementary PNA (DNA) microarray probe was 5′ terminated with the spacer (NH2-C6) and anchored to the agarose substrate by means of the N (amine group of spacer) and C (carbon of agarose) bond; the obtained systems were solvated by adding water molecules.

The simulations were performed employing the Amber 99 Parmbsc force field,[28] the treatment of solvent molecules and the equilibration procedure adopted were reported in Ref.[29] All the simulations were run with Gromacs 2020 series under Periodic Boundary Condition using the NPT ensamble (P = 1 atm) at 298 and 333 K and a time step of 1 fs was applied to integrate the equation of motion. We have used the following geometric criteria for the definition of a hydrogen bond: a) the hydrogen-acceptor distance < 2.5 Å, b) the donor-hydrogen-acceptor angle > 90°.

3 | RESULTS AND DISCUSSIONS

3.1 | Substrate preparation and characterization

The proposed microarray system consists of a hybridization micro reactor with a multilayer components Si/Al/agarose, properly conceived to anchor PNA microarray probes on agarose layer and to achieve fluorescence enhancement by constructive interference of fluorophore emission (Cy5). The microarray substrate was composed of a multilayer structure comprising a silicon support, a mirror layer (Al-Si-Cu) produced by CVD method and spin-coated agarose layer (Figure 1). The agarose thickness was properly tuned by tuning the coating deposition speed, as showed in Figure 1, varying the deposition speed from 300 to 1000 rpm for 60 s at temperature of about 75°C, to obtain a uniform coating with the follow thickness values: 800 ± 15 nm, 830 ± 20 nm, 900 ± 22 nm, and 1000 ± 25 nm.

To investigate the optical performance of microarray substrate, samples consisting of Cy5-target spot (at final concentration of 50 nM) were printed on substrates with agarose thicknesses values of from 800 to 1000 nm, the fluorescence signals at 650 nm were acquired immediately after spotting process, obtaining the following values: 9000 ± 300 a.u. (800 nm), 10,000 ± 400 (830 nm), 15,000 ± 500 a.u. (900 nm), and 7000 ± 500 a.u. (1000 nm). The fluorescence signals (15,000 ± 500 a.u.) show a maximum of emission corresponding to an agarose thickness value of about 900 nm (Figure 1B). At this value of agarose thickness a fluorescence probe density value of 2.500 PNA μm^{-2} was calculated.

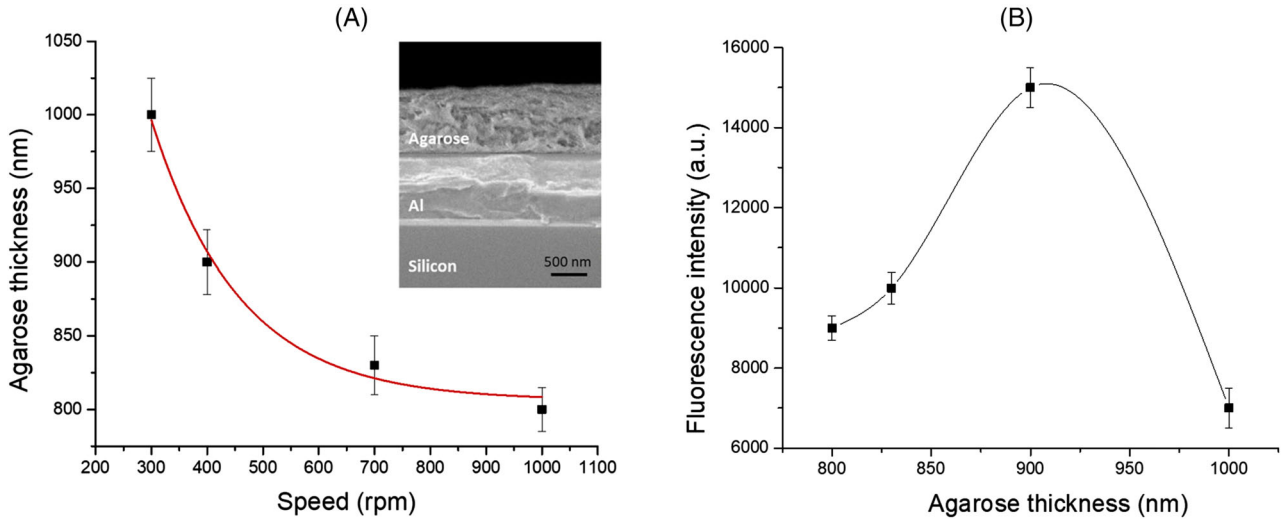

FIGURE 1 Agarose coating thickness versus spin coating speed (insets the representative SEM micrographs for cross profile of the layered Si/Al/Agarose substrate (A) and Cy5 emission signal versus agarose thickness (B)

3.2 | PNA Microarray preparation

In order to link the amino-terminated PNA probes to the agarose surface, a multi-step steps approach based on oxidation-Schiff's base-reduction was used. In details, to promote the oxidation of two vicinal hydroxyl groups of agarose layers to form reactive aldehydes terminations, an activation reaction in HIO_4 for 30 min at room temperature was performed. The FTIR investigation for untreated agarose coating shown the bands at 3350 cm^{-1} (O-H_stretch band) and at 1050 cm^{-1} (C-O_stretch band), while the FTIR spectrum for the activated agarose coating shows the typical bands of aldehydes termination, in particular a sharp band at 1738 cm^{-1} (C = O stretch,) and at 2967 cm^{-1} (= C-H_stretch band), see figure ESI.

The effectiveness of the agarose film formation and the activation process was also confirmed by the water contact angle measurements. After cleaning process, contact angle values of about 10° was measured on Al surface, as expected for a hydrophilic surface. After spin coating deposition of the agarose film, a contact angle value of 27.5 ° ± 1.0 was recorded, then a change of wettability surface property was obtained after oxidation with $NaIO_4$ (21.5° ±1.1), to demonstrate the effectiveness of the activation reaction. The agarose activation is aimed to improve the covalently reaction between the oligonucleotide amino termination with agarose aldehyde groups to form the Schiff's base. A 4 × 6 PNA-microarray was printed on activated agarose surface and then the substrate was incubated for 4 h at 30°C and relative humidity 90%. Then, the substrates were immersed in reducing $NaBH_4$ solution, rinsed with deionized water and dried. The PNA microarray fabrication and testing is schemed in SI section.

3.3 | miRNA recognition

In order to assess the performance of the PNA-microarray system on miRNA122 recognition, ten replicates were tested for each target amount (0.1, 0.5, 5.0, 10.0, 25.0, and 50.0 nM). In Figure 2A and 2B the representative microarray-spots optical image and fluorescence hybridization images are reported. The fluorescence signal profile for the hybridized positive control (CTRL+), negative control (CTRL-) and specific miRNA_122 spots is depicted in Figure 2C. All probe sequences are reported in Section 2.

In order to evaluate the limit of detection (LoD) and the limit of background (LoB) values for miRNA-122, the linear regression method has been applied. The LoB value has been obtained by equation LoB = [NB(p/100) + 0.5], in which NB is number of background replica and estimating the 95% percentile p = (100-α) = 95. From this procedure was obtained a LoB values of about 25 The LoD was estimated set to four times the LoB signal intensity value in the regression linear Equation Y = 25+1750X, obtaining a LoD value of about 43 pM. Regarding the sensitivity, it was defined as the slope of the regression linear equation a value of about 1.75 μM^{-1}. To ascertain a good probe immobilization efficiency, the hybridized-site density value was calculated by fluorescence signals at various labeled probe amount. The value calculated was about 800 ±20 U μm^{-2}.

The second part of our experimental investigation was focused on the calculation of association constant K_{ass}, between the PNA-probe and the miRNA122 target. This was calculated by means of the Langmuir isotherm model. Figure 2D reports the linear plot of ratio $I/(I_{max}\text{-}I)$ versus the molar concentration of miRNA_122 target.

The association constant was obtained from the slope of the linear region 0.1–10 nM according to the equation reported in Section 2.6. The Fluorescence intensity values obtained were: 0.035 ± 0.1 (0.1 nM), 0.177 ± 0.1 (0.5 nM), 0.507 ± 0.12 (5 nM), 0.935 ± 0.13 (10 M). The value of the association constant was found 8 × 10^7 M^{-1}. This result is in accordance to the typical K_{ass} reported in literature for hybrid PNA-RNA duplex (ranging from 10^6 to 10^9 M^{-1}, depending on the target sequence and substrates).

In order to investigate the specificity of the assay, hybridization experiments were carried out interrogating the microarray with

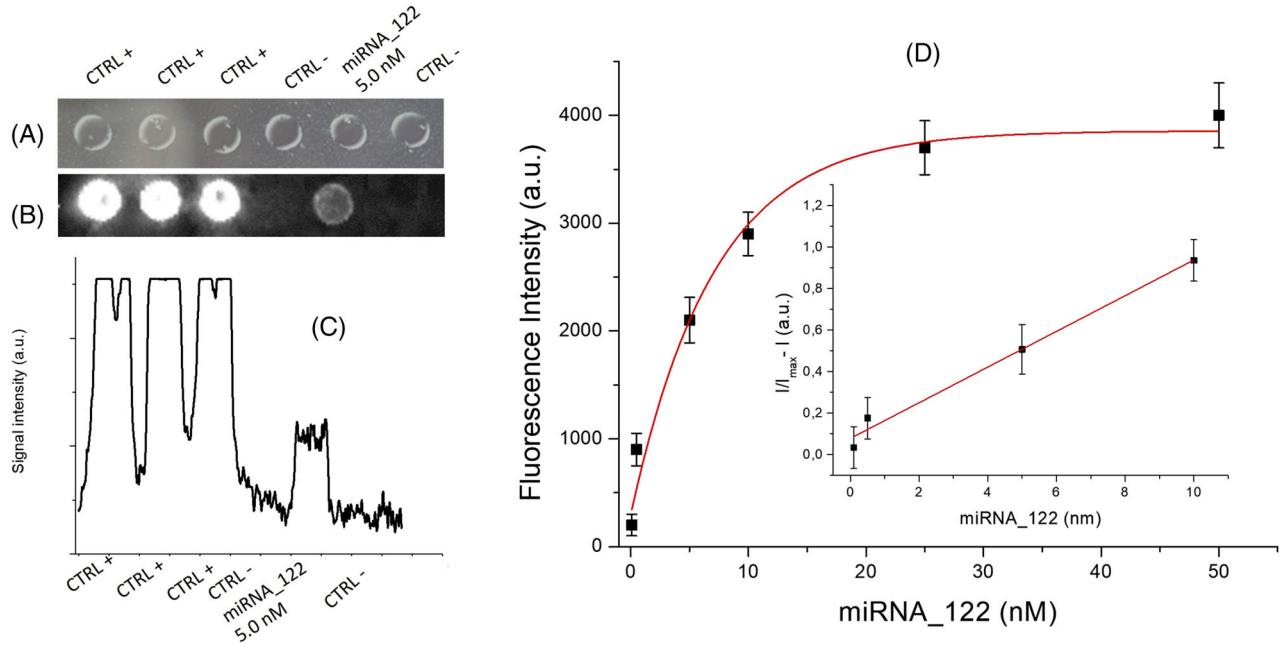

FIGURE 2 PNA-microarray experiments: A) representative PNA-microarray spots optical images, B) representative fluorescence hybridization images, C) hybridization plot profile signal of hybridized spots and D) Langmuir isotherm plot for PNA-miRNA_122 duplex (Inserted the linear regression for the calculation of $K_{ass} = 8.0 \times 10^7\ M^{-1}$, $R^2 = 0.997$)

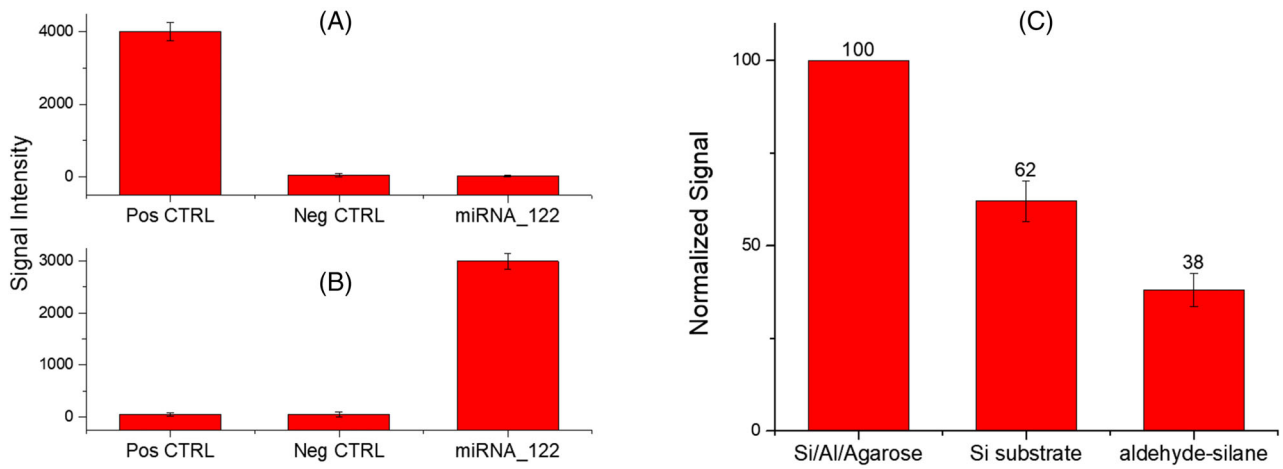

FIGURE 3 Hybridization experiments: A) specificity tests performed with specific target Pos_CTRL (signal 3925 ±207) and unspecific targets (Neg CTRL 48±14, *p*-value 3.7×10^{-8}) and miRNA122 (49 ±17, *p*-value 3.7×10^{-8}), B) specificity tests performed with specific target miRNA_122 (2980 ± 192,) and unspecific targets CTRL Neg (64±12, *p*-value 1.4×10^{-7}) and Pos_CTRL (44±8, *p*-value 1.4×10^{-7})C) hybridization responses for various coated substrates: Si/Al/agarose 100% (3100 a.u.) silicon 62 ± 5.6%, 1920 a.u. (*p*-value 2.09×10^{-4}) and aldehyde-coating glass slide 38 ± 4.6%, 1178 a.u. (*p*-value 1.29×10^{-5})

specific and unspecific targets. The results, summarized in Figure 3A and B. In detail, the specificity tests were performed interrogating the PNA-microarray with specific targets (pos_CTRL, miRNA_122) and unspecific targets (Mis-target). The results clearly confirm a good specificity for the PNA microarray assay.

In order to demonstrate the improvement effect of agarose coating hybridization experiments using specific miRNA_122 target (200 nM) were performed on agarose-free substrates such as silicon and aldehyde-coating glass slide. The results depicted in Figure 3C showed that the hybridization signal for silicon substrate was just the 62 ± 5.6% respect the value for the agarose signal (100% while the hybridization signal measured on aldehyde-coating glass slide was lower (about 38 ± 4.6%..).

The third part of our experiments was intended to assess the capability of our PNA microarray system to detect the miRNA-122 directly on biological samples. At this regard, human serum samples

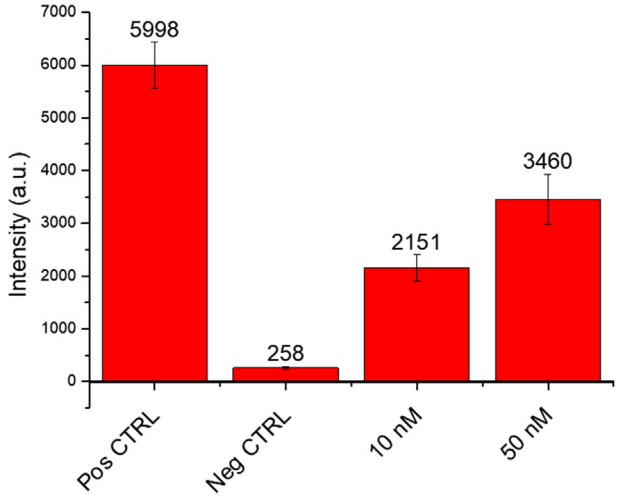

FIGURE 4 miRNA_122 recognition in human serum samples: microarray hybridization signals for positive CTRL (5998 ± 436 a.u.), negative CTRL (258 ± 329 a.u.), and specific miRNA_122 target at 10 nM (2151 ± 252 a.u.; *p*-value $1.71*10^{-7}$) and 50 nM (460 ± 472 a.u.; *p*-value $3.60*10^{-7}$)

TABLE 2 main miRNA-assays

miRNA detection assay	LoD	Refs.
Dynamic Chemical Labeling	1.32 pM	[30]
PNA-RNA hybridization	100 pM	[31]
Single molecule array	500 fM	[32]
SplintR Ligase.	2-4pgr	[33]
miR-122: TaqMan MicroRNAAssay(LIFE technololy)	1-10 ngr	[34]

were spiked with various amounts of miRNA-122 (10 and 50 nM) and tested, each sample was replicated five times. The hybridization signals for miRNA specific probes, at concentration of 10 nM, was 2151±252 a.u. (*p*-value $1.71*10^{-7}$), 50 nM, 3460 ± 472 a.u. (*p*-value $3.60*10^{-7}$), while for the positive and negative hybridization controls were 5998±436 a.u. and 258±329 a.u., respectively. These data demonstrated that our PNA-microarray system can successful detect miRNA122 targets in human serum sample (Figure 4).

Various technologies have been recently proposed for miRNA detection (Table 2). Recently, Dynamic Chemical Labeling for miRNA_122 detection has been proposed by Diaz–Mochon and coworkers.[30] This assay specifically measured miR-122 directly from human serum or plasma without extraction and amplification steps, with a limit of detection of 1.32 pM for the identification of drug-induced liver injury. The same research team has developed a simple method for detection of miRNA_122 in human serum without PCR amplification, achieving a limit of detection of 100 pM. The method is based on hybridization of miRNA target with PNA probe and detection using fluorescence measurements.[31] An analogous PCR-free approach based on Single-Molecule array based on PNA-probe was proposed for directly miRNA_122 detection on human serum, reaching a limit of detection of 500fM.[32] Jin et al. proposed the SplintR Ligase method based on a two-step approach which involves a ligation of

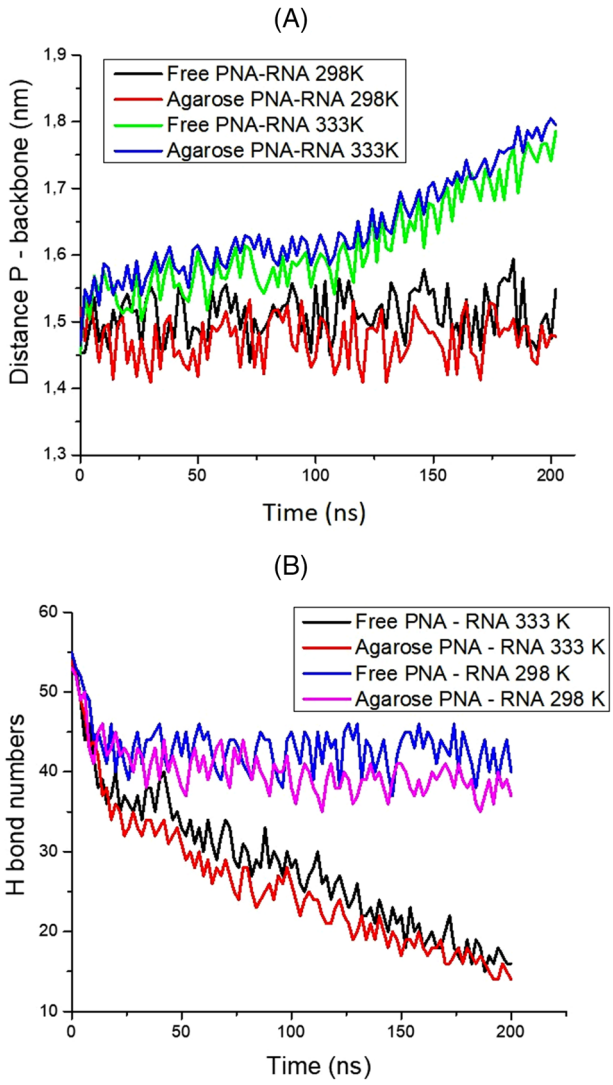

FIGURE 5 (A) Time fluctuation of the backbone distance for free PNA-RNA and Agarose-PNA-RNA at 298 and 333 K and (B) Temporal profiles of number of H-bonds between the strands at 298 and 333 K

miRNA target by DNA probe followed by optical real-time quantitative PCR quantification, reaching a limit of detection of 2–4 pg.[33] The TaqMan MicroRNA Assay (LIFe technology) is a commercially available kit for miRNA_122 detetction based on microRNA Reverse Transcription Kit for miR-122 and TaqMan Universal qPCR reaching a limit of detection of 1–10 pg.[34]

3.4 | MD simulation of probe-target interaction on agarose substrate

The initial structures of free and agarose-linked dsPNA-RNA and dsDNA-RNA, obtained as reported in the methods, were equilibrated at 298 K (room temperature) and 333 K (hybridization temperature) running, respectively, 3 and 5 ns NPT molecular dynamics. Hence, 200 ns productive run was performed maintaining the NPT ensemble at different temperature. In Figure 5A we report the backbone

distance, bd, between dsPNA-RNA at 298 and 333 K with agarose and without agarose (free). The average trend shows, for the lowest temperature (298 K), a bd value of about 1.45 nm for the free-agarose system and a value of 1.52 nm for the agarose-dsPNA-RNA suggesting a contribute due to the agarose structure to the dsPNA-RNA duplex interaction. While, at higher temperature (333 K), the double strand dissociation takes place as indicated by the increase of the bd values (especially after 100 ns): here the role of agarose on chain separation is more evident with higher bd values, of about 0.1 nm (Figure 4A blue line).

Similar results were found in the analysis of DNA–RNA systems; in these cases, however, the values of the reference parameter bd indicate that the PNA tends to stabilize the double strand; indeed the values obtained in the DNA–RNA duplex are significantly greater than those evaluated for ds–PNA–RNA (ESI). Such findings indicate the higher stability of the PNA–RNA hybrids compared to DNA–RNA double strand that is negatively charged, as widely reported in literature[34] and as confirmed by our previous hybridization experiments conducted interrogating PNA and DNA probes with RNA target amount of 15 nM. We obtained a fluorescence signal value for the hybridization PNA-RNA (2200 ± 150 a.u.) higher than those obtained for the DNA-RNA hybridization (1800 ± 100 a.u.). PNA lacks charges and consequently during hybridization with RNA or DNA strands lacks electrostatic repulsion offering a greater affinity toward the complementary target. The PNA recognizes complementary sequences of RNA (or DNA) following the Watson–Crick base-pairing. As showed above, the increasing of temperature induces the duplex dissociation due to the loss of hydrogen bonds. Such effect is reported in Figure 5B which shows the amount of hydrogen bonds for both systems at 298 and 333 K from 0 to 200 ns. At lower temperature (298 K) the H-bond average value decrease reaching a final value of 40 ±2 U, after 25 ns, for the agarose-PNA-RNA system and about 44 ±2 U for the free-PNA-RNA.

Indeed, the smaller number of H-bonds observed in the case of agarose complex still suggests that the surface influences the duplex stability by weakening the interstrand hydrogen bonds. The degree of -OH coverage of a surface has been showed to influence the hydrogen bond strength of substrate interacting with the surface itself,[38] thus we consider that such effect can be invoked to explain the role of the highly OH covered agarose surface in the ds PNA-RNA stabilization. At higher temperature, the number of bonds decreases from the starting value of 54 ± 2 U with a Kdec value of 0.013 ± 0.0013 ns^{-1} for agarose-ds-PNA-RNA system and K_{dec} value of 0.0056 ± 0.0019 ns^{-1} for free ds-PNA-RNA, reaching the final values of 13 and 16 U, respectively, at the end of the simulation (ESI). Noteworthy, in all cases (298 and 333 K), the amount of hydrogen bond starts to decrease from the beginning of the simulation and is faster in the DNA-RNA cases compared to the hybrid-PNA analogs (ESI). Whereas, consistently, lower values are found for agarose dsDNA-RNA. Moreover, in order to evaluate the contribution of each base pairing to the double strand stability we have considered the fraction of the simulation time (%) during which the base pairs remain H-bonded at different temperatures (Figure 6A and B).

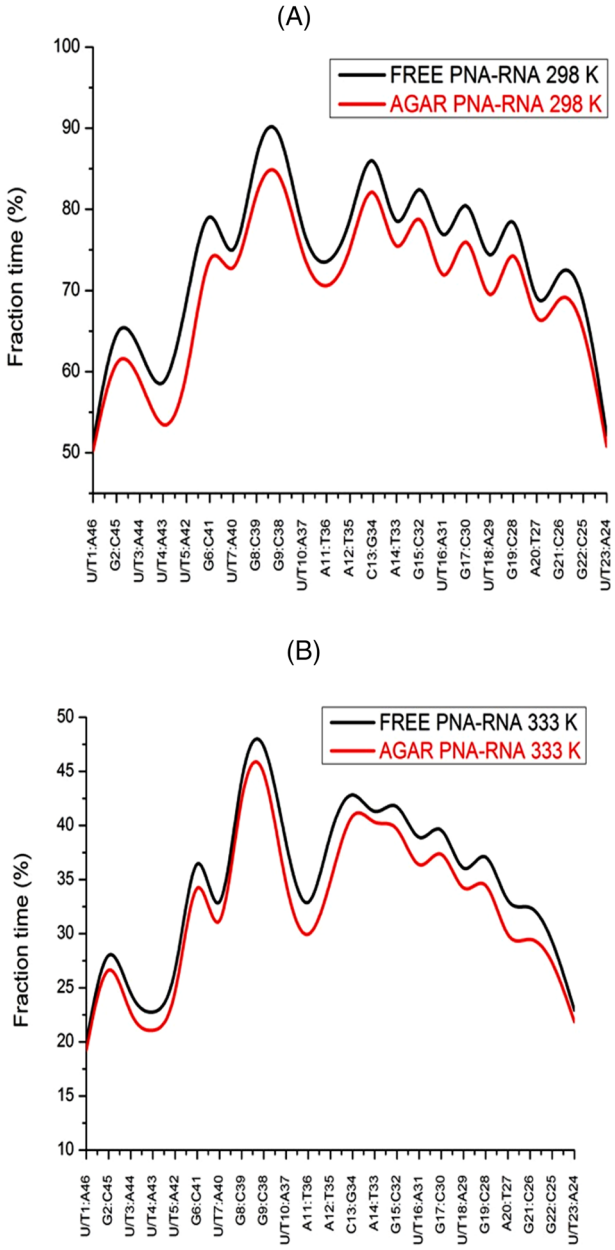

FIGURE 6 Fraction of the MD simulation time (measured at 200 ns) during which individual base pairs remained WC hydrogen bonded in the duplex PNA-RNA models at (A) 298 K and (B) 333 K

At lower temperature, excluding terminal residues, the fraction time calculated for each base pair of free-ds PNA-RNA remains over 60% during the simulation time. Slight lower values of this parameter were instead calculated in the agarose-dsPNA-RNA system (Figure 6A). In particular, it has to be emphasized that in the near 3′ terminal UUU triplet the fraction time drops below 55%. In general A:U base pairs are more loosely bound than G:C base pairs as the form only two H-bonds whereas guanine and cytosine form three H-bonds, furthermore near terminal position H-bonds are easily broken compared to central H-bonds. In any case, at 298 K the H-bonds between base pairs are persistent and stabilize the double stranded structure. At higher temperature (333 K) we observe that mostly H-bonds are broken after

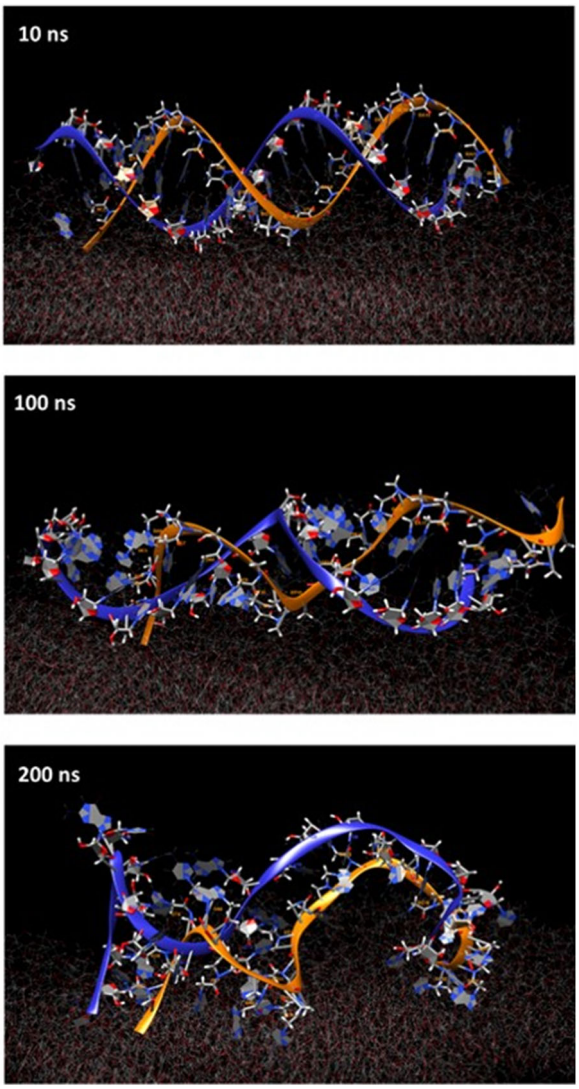

FIGURE 7 PNA-RNA duplex de-hybridization process on agarose surface after 10, 100, and 200 ns at 333K

200 ns, the fraction time decreases at less than 50% for all the strands; remarkably H-bonds involved in G8G9 duplet are more persistent showing the higher values of the parameter (about 45%). Moreover, in this case the fraction time for the agarose-dsPNA-RNA system is lower than for the free system to indicate a clear contribution of the agarose substrate on dsPNA-RNA interaction. Recently, we have shown that the presence of central triplets, or doublets, featured by a consecutive sequence of guanine or cytosine, gives rise to a cooperative effect that contributes to the stabilization of a duplex as temperatures rises. In the studied sequence, the only contribution of the G8G9 duplet is too weak to stabilize the double strand at higher temperature.

Figure 7 reports the simulation of PNA-RNA duplex de-hybridization process on agarose surface after 10 ns, 100 ns, and 200 ns at temperature of 333 K. Undoubtedly, it indicates that the double stranded PNA-RNA starts the denaturation at 100 ns while after 200 ns it could be considered abundantly dehybridized.

Finally, the modeling simulations showed that the agarose substrate gives a contribution to the ds PNA–RNA interactions either for the lower temperature (298 K), either for the hybridization condition (333 K), resulting on a decrease of H-bonds amount for the ds PNA–RNA system on the agarose surface. These data suggest that the nature of the substrate can influence the hybridization efficiency and can increase it by tuning the amount of H-bond unit between the double strands.

4 | CONCLUSIONS

In this work, a novel PNA–microarray substrate based on multilayers for miRNA recognition has been proposed. The substrate contains a multilayer structure consisting of a silicon support, an aluminum film acting as a light mirror and a finishing agarose layer. The effectiveness of the proposed system in regard to the hybridization processes and signal acquisition was investigated in the detection of miRNA target showing a sensitivity of about 1750 nM^{-1}, and a LoD of about 0.043 nM, as a function of the capture probe sequence.

The evaluation of the coupling process effectiveness by means of the Langmuir isotherm model gave an association constant (K_{ass}) value of about 8.0×10^7 M^{-1}.

Modeling simulations indicate that the agarose substrate gives a remarkable positive contribution to the ds PNA–RNA interactions, especially in the direction to avoid any potential nonspecific interaction.

All these results clearly show that this substrate is very promising in the development of new microarray platforms for the next generation of molecular diagnostic devices. Further studies will include additional substrates and surface chemistry to better represent the effect of the agarose on PNA–RNA hybridization (see Supporting Informartion).

ACKNOWLEDGMENTS

Special thanks to Dr. Salvatore Pernagallo for his support on PNA probe design, Dr. Enrico Alessi for his support on optical characterization and Dr. Maria Anna Messina for the statistical analysis.

CONFLICT OF INTEREST

The authors declare no commercial or financial conflict of interest.

DATA AVAILABILITY STATEMENT

Research data are not shared.

ORCID

Salvatore Petralia https://orcid.org/0000-0001-5692-1130

REFERENCES

1. Miller, M. B., & Tang, Y.-W. (2017). Basic concepts of microarrays and potential applications in clinical microbiology *Clinical Microbiology Reviews Journal*, *22*, 611–633.
2. Gunderson, L. K., Steemers, F. J., Lee, G., Mendoza, L. G. & Chee, M. S. (2005). A genome-wide scalable SNP genotyping assay using microarray technology *Nature Genetics*, *37*, 549–554.
3. Petralia, S., Verardo, R., Klaric, E., Cavallaro, S., Alessi, E., & Schneider, C. (2013). In-Check system: A highly integrated silicon Lab-on-Chip

for sample preparation, PCR amplification and microarray detection of nucleic acids directly from biological samples *Sensors and Actuators B: Chemical*, *187*, 99–105.
4. Cao, B., Wang, S., Tian, Z., Hu, P., Feng, L., & Wang, L. (2015). DNA microarray characterization of pathogens associated with sexually transmitted diseases *Plos One*, *10*, e0133927.
5. Hardiman, G. (2008). *Methods in Molecular Biology*, *448*, 21–30.
6. Russo, G. I., Musso, N., Romano, A., Caruso, G., Petralia, S., Lanzanò, L., Broggi, G., & Camarda, M. (2022). The role of dielectrophoresis for cancer diagnosis and prognosis. *Cancers*, *14*, 198.
7. Feng, J., Wang, Y., Jin, R., & Hao, G. (2020). A universal random DNA amplification and labeling strategy for microarray to detect multiple pathogens of aquatic animals. *Journal of Virological Methods*, *275*, 113761.
8. Cao, L., Guo, X., Mao, Pi., Ren, Y., Li, Z., You, M., Hu, J., Tian, M., Yao, C., Li, F., & Xu, F. (2021). A portable digital loop-mediated isothermal amplification platform based on microgel array and hand-held Reader. *ACS Sensors*, *6*, 10, 3564–3574.
9. Li, Z., Bai, Y., You, M., Hu, J., Yao, C., Cao, L., & Xu, F. (2021). Fully integrated microfluidic devices for qualitative, quantitative and digital nucleic acids testing at point of care. *Biosensors and Bioelectronics*, *177*, 112952.
10. Ventimiglia, G., & Petralia, S. (2013). Recent advances in DNA microarray technology: An overview on production strategies and detection methods. *BioNanoScience*, *3*, 428–450.
11. Petralia, S., & Ventimiglia, G. (2014). A facile and fast chemical process to manufacture epoxy-silane coating on plastic substrate for biomolecules sensing applications. *BioNanoScience*, *4*, 226–231.
12. Petralia, S., Ventimiglia, G., Ceschia, S., Gasparin, M., & Verardo, R. (2017). A novel silver coating for antigen-microarray preparation suitable for application on antibody recognition. *BioNanoScience*, *7*, 449–455.
13. Ventimiglia, G., Alessi, E., & Petralia, S. (2016). A bridge-like solution for Universal Microarray applications. *Sensors and Actuators B*, *232*, 102–106.
14. Koch, C. A., Li, P. C. H., & Utkhede, R. S. (2005). Evaluation of thin films of agarose on glass for hybridization of DNA to identify plant pathogens with microarray technology *Analytical Biochemistry*, *342*, 93–102.
15. Mayer, M., Yang, J., Gitlin, I., Gracias, D. H., & Whitesides, G. M. (2004). Micropatterned agarose gels for stamping arrays of proteins and gradients of proteins *Proteomics*, *8*, 2366–2376.
16. Li, L., Wang, W., Ding, M., Luo, G., & Liang, Q. (2016). Single-cell-arrayed agarose chip for in situ analysis of cytotoxicity and genotoxicity of DNA cross-linking agents. *Analytical Chemistry*, *88*, 6734–6742.
17. Hayes, J., Peruzzi, P. P., & Lawler, S. (2014). MicroRNAs in cancer: Biomarkers, functions and therapy. *Trends in Molecular Medicine*, *20*, 460–469.
18. Condrat, C. E., Thompson, D. C., Barbu, M. G., Bugnar, O. L., Boboc, A., Cretoiu, D., Suciu, N., Cretoiu, S. M., & Voi, S. C. (2020). miRNAs as biomarkers in disease: latest findings regarding their role in diagnosis and prognosis. *Cells*, *9*, 276.
19. Sardiello, M., Palmieri, M., Di Ronza, A., Medina, D. L., Valenza, M., Gennarino, V. A., Di Malta, C., Donaudy, F., Embrione, V., Polishchuk, R. S., Banfi, S., Parenti, G., Cattaneo, E., & Ballabio, A. (2009). A gene network regulating lysosomal biogenesis and function. *Science*, *325*, 473–477.
20. Momen-Heravi, F., & Bala, S. (2016). *Molecular Aspects of Alcohol and Nutrition*, *22*, 275–286.
21. Zhou, X., Fang, S., Wang, M. A., Xiong, Zheng, C., Wang, J., & Yin, C. (2019). Diagnostic value of circulating miRNA-122 for hepatitis B virus and/or hepatitis C virus-associated chronic viral hepatitis. *Bioscience Reports*, *39*, BSR20190900.
22. Starkey Lewis, P. J., Dear, J., Platt, V., Simpson, K. J., Craig, D. G. N., Antoine, D. J., French, N. S., Dhaun, N., Webb, D. J., Costello, E. M., Neoptolemos, J. P., Moggs, J., Goldring, C. E., & Park, K. (2011). Circulating microRNAs as potential markers of human drug-induced liver injury. *Hepatology*, *54*, 1767–1776.
23. Zhang, N., Appella, D. H. (2010). Advantages of peptide nucleic acids as diagnostic platforms for detection of nucleic acids in resource-limited settings. *Journal of Infectious Diseases*, *201*, S42–S45.
24. Kim, H., Choi, J., Cho, M., & Park, H. (2012). A PNA microarray platform for miRNA expression profiling using on-chip labeling technology. *BioChip Journal*, *6*, 25–33.
25. Pernagallo, S., Ventimiglia, G., Cavalluzzo, C., Alessi, E., Ilyine, H., Bradley, M., & Diaz-Mochon, J. J. (2012). Novel Biochip Platform for Nucleic Acid Analysis *Sensors*, *12*, 8100-8111.
26. Zhang, H., Liu, X., Zhang, C., Xu, Y., Su, J., Lu, X., Shi, J., Wang, L., Landry, M. P., Zhu, Y., Lv, M., & Mi, X. (2020). A DNA tetrahedral structure-mediated ultrasensitive fluorescent microarray platform for nucleic acid test, *Sens. Actuators*, *B*, 128538.
27. Ventimiglia, G., Petralia, S., & Alessi, E. (2012). *Sensors & Transducers Journal*, *139*, 152–161.
28. Ivani, I. (2016). Parmbsc: A refined force field for DNA simulations *Nature Methods*, *13*, 55–58.
29. Lindahl, E., Abraham, M., Hess, B., & Van der Spoel, D. (2021). *GROMACS 2020.6 Manual*, 2021.
30. López-Longarela, B. (2020). Direct detection of miR-122 in hepatotoxicity using dynamic chemical labeling overcomes stability and isomiR challenges *Analytical Chemistry*, *92*(4), 3388–3395.
31. Fernandez, E. G. (2019). *Chemical Communications*, *55*, 14958–14961.
32. Rissin, D. M., López-Longarela, B., Pernagallo, S., Ilyine, H., Vliegenthart, A. D. B., & Dear, J. W. (2017). Polymerase-free measurement of microRNA-122 with single base specificity using single molecule arrays: Detection of drug-induced liver injury. *Plos One*, *12*, e0179669.
33. Jin, J., Vaud, S., Zhelkovsky, A. M., Posfai, J., & L, A. (2016). Sensitive and specific miRNA detection method using SplintR Ligase. *McReynolds Nucleic Acids Research*, *44*, e116.
34. https://www.thermofisher.com/
35. Pellestor, F., & Paulasova, P. (2014). The peptide nucleic acids (PNAs), powerful tools for molecular genetics and cytogenetics. *European Journal of Human Genetics*, *12*, 694–700.
36. Lundin, L. K., Hasan, M., Moreno, P. M., Törnquist, E., Oprea, I., Svahn, M. G., Simonson, E. O., & Smith, C. I. (2005). Increased stability and specificity through combined hybridization of peptide nucleic acid (PNA) and locked nucleic acid (LNA) to supercoiled plasmids for PNA-anchored -Bioplex- formation. *Biomolecular Engineering*, *22*, 185–189.
37. Swenson, C. S., Lackey, H. H., EJ, R., Harris, J. M., Heemstra, J. M., & Peterson, E. M. (2021). Evaluating the effect of ionic strength on PNA:DNA duplex formation kinetics. *RSC Chemical Biology*, *2*, 1249–1256.
38. Consiglio, G., & Forte, G. (2018). Molecular dynamics study of coil-to-globule transition in a thermo-responsive oligomer bound to various surfaces: Hydrophilic surfaces stabilize the coil form. *Physical Chemistry Chemical Physics*, *20*, 9754–29763.

SUPPORTING INFORMATION

Additional supporting information may be found in the online version of the article at the publisher's website.

How to cite this article: Forte, G., Ventimiglia, G., Pesaturo, M., & Petralia, S. (2022). A highly sensitive PNA-microarray system for miRNA122 recognition. *Biotechnology Journal*, *17*, e2100587. https://doi.org/10.1002/biot.202100587